Thinnest Uniform Liquid Films Formed at the Highest Speeds with Reverse Roll Coating

H. Benkreira
School of Engineering, Design and Technology, University of Bradford, Bradford, West Yorkshire, UK

Y. Shibata
School of Engineering, Design and Technology, University of Bradford, Bradford, West Yorkshire, UK

Films R&D Centre, Toyobo Co. Ltd., Otsu, Japan

K. Ito
Films R&D Centre, Toyobo Co. Ltd., Otsu, Japan

DOI 10.1002/aic.14060
Published online March 11, 2013 in Wiley Online Library (wileyonlinelibrary.com)

Reverse roll coating is probably the most widely used coating operation, much less investigated than its counterpart and inherently unstable forward roll coating. A new data to complement earlier work which was limited to large gaps and thus "thick" films is presented. The intention is to assess the feasibility of reverse roll coating to yield very thin films (<10 μm) at high speeds (>1 m/s) for application in the newer technologies, such as the production of solar cells and plastic electronics. The data obtained demonstrate this is possible but at the lowest permissible gap (25–50 μm) with low-viscosity fluids (∼7 mPa s). The study also developed a new understanding of how instabilities are controlled. It was seen that the size of the inertia forces generated by the applicator roller in relation to surface tension, as expressed by the Weber number and not the applicator Capillary number (viscous forces/surface tension) which is the critical parameter. © 2013 American Institute of Chemical Engineers *AIChE J*, 59: 3083–3091, 2013
Keywords: reverse roll coating, thin films, instabilities, ribbing

Introduction

Reverse roll coating is probably the coating operation most widely used in industry to deposit thin films of liquid for decorative, protective, or functional applications. Examples of applications are numerous and include the coating of paper for printability, the coating of plastic films to produce photographic films, medical X-rays, audio and video magnetic tapes, electronic printed circuits, controlled release medical drug substrates, the coating of metal foils, and textile sheets. Coated products pervade through the economy of our modern age and the drive for higher productivity pushes towards higher throughput (coating speed), thinner films and stricter requirements on surface uniformity whilst keeping the principle of operation and equipment simple, versatile and cheap. This article deals precisely with these aspects by revisiting the fluid mechanics of reverse roll coating, a simple coating operation, and assessing its adaptability to the new technologies being developed currently in the electronic and energy sectors such as solar cells and plastic electronics. Both examples require uniform liquid films of thickness less than 5 μm to be produced at roll speeds higher than 1 m/s. These production targets effectively push the limits of coating thin liquid films to near submicron scales and represent the scientific challenges addressed in this article.

In its simplest configuration (see Figure 1), the reverse roll coating operation consists of two co-rotating rollers separated by a gap, an applicator roller partially immersed in a trough containing the coating liquid and a metering roller, placed usually directly above or at an angle. Typically, the rollers radius, R, and gap, h_0, are in the range 15–30 cm and 100–500 μm, respectively. The applicator roller, which rotates at speed V_A picks-up from the trough a thin film of thickness h_A which is metered by the metering roller, rotating opposite at speed V_M, normally of magnitude 10–20% V_A. This simple coating flow results in a film of thickness h_M, smaller than both h_A and h_0, formed at speed V_A on the applicator roller. Better controlled arrangements of this simple flow may include a doctor blade (see Figure 1) metering the arriving film so that the gap is not flooded and an even more effective metering ensues, resulting in principle with a thinner metered film. Variations on this premetering are many and may include a third stationary or rotating roller metering the film taken by the applicator roller from the trough. As for the transfer of the final metered film onto the substrate to be coated, an additional rubber covered roller is normally used (see Figure 1). The substrate is wrapped around this deformable roller which is in kiss-contact with the applicator roller.

Correspondence concerning this article should be addressed to H. Benkreira at H.Benkreira@bradford.ac.uk.

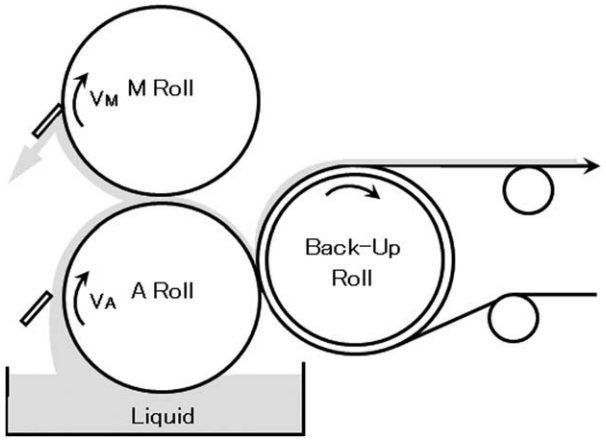

Figure 1. Schematic configuration of reverse roll coating.

[Color figure can be viewed in the online issue, which is available at wileyonlinelibrary.com.]

Clearly, as reverse roll coating is a flow metered by a gap, the limit on film thickness is dictated by how small a gap the coater can be operated at. To avoid rollers clashing and to work within the limits of roller machining accuracy (typically not better than 2 μm), operation with rigid rollers below a 25 μm gap and producing films thinner than about 10 μm is not feasible practically. This explains why the bulk of previous work (reviewed below) has been carried out at large gaps (100–1000 μm). The aim of this article is to report on work within lower gap limits down to 25 μm with a view of developing further the potential of reverse roll coating and to adapt it to the newer requirements of very low film thickness and high speeds. No prior work *per se* has been done in these limits; however, previous research gives helpful indications as is described below.

The fluid mechanics of reverse roll coating, in terms of how the metered film thickness (the important design and operation information) varies with operating conditions has been well researched. Ho and Holland[1] were probably the first to present an analysis of the flow, based on the lubrication approximations, and predicted that the net flux of fluid exiting the gap and forming the metered film was related with operating conditions as

$$q_M = V_A h_M = \frac{2}{3} h_0 (V_A - V_M) \quad (1)$$

Expressed in dimensionless form, the above equation gives the dimensionless metered film thickness H_M ($=h_M/h_0$) as a linear function of the metering roller speed to applicator roller speed ratio r_S ($=V_M/V_A$)

$$H_M = \frac{2}{3}(1 - r_S) \quad (2)$$

This equation implies that the physical properties of the fluids have no effect, a most desirable feature for industrial purposes. Clearly, as the lubrication approximation assumes the flow to be one dimensional, this result will apply strictly only when $V_A >> V_M$ or $r_S << 1$ and of course when the fluid is Newtonian. To verify their prediction, Ho and Holland[1] carried out a few experiments at large gaps (305–458 μm) and small applicator speeds (0.05–0.30 m/s) and with a high viscosity fluid (750 mPa s). The fit between their data and Eq. 1 was excellent. Following from this work, Benkreira et al.[2] presented a large range of data that supported Eq. 1 and extended its applicability to non-Newtonian purely viscous liquids but again with the limitation that the gaps were large (>200 μm) and speed low (<0.80 m/s). Both Ho and Holland[1] and Benkreira et al.[2] worked within the limit of the lubrication approximation with $r_S < 1$ and did not report on the surface instabilities that may arise.

Years later, Coyle et al.[3] revisited this problem theoretically, making use of the advent of powerful computers and advances in computational fluid dynamics (CFD) modeling that were being developed at the time at the University of Minnesota. His finite elements analysis enabled resolving the strong 2D aspect of this flow with no bounds on the speed ratio r_S and full consideration of the free surfaces that formed upstream and downstream including the dynamic wetting line. Their analysis now included the important capillary number, Ca ($=\mu V_A/\sigma$), a measure of the relative extent of viscous forces to surface tension forces and the contact angle θ_C that the dynamic wetting line forms with the metering roller. The predictions that Coyle et al.[3] obtained confirmed the earlier results of Ho and Holland[1] and Benkreira et al.[2] but went further in that they covered the effects of Ca and speed ratio over a much larger range (some simulations were performed at V_M/V_A up to 2.5). This important work revealed that the linear decrease of H_M with r_S held only in a range of speed ratios, 0–r_S^* with a turning point at the critical speed ratio r_S^*, where H_M rises nonlinearly as r_S is increased further beyond r_S^*. It was further observed that the larger the capillary number Ca the smaller was the critical speed ratio r_S^*. Figure 2a illustrates this rather perplexing variation of H_M which is explained as being the result of the dynamic wetting line moving into and passed the minimum gap position (see Figure 2b). As this occurs, the actual metering gap is no longer h_0 but a larger value hence the observed increase in the metered film thickness. Clearly, how well the model of Coyle et al.[3] was at tracking this critical region determined the goodness of fit between their CFD predictions and measured data. As it is in this region that the metered film forms from the dynamic wetting line position, the conditions imposed on this line are critical. As there are uncertainties on the exactness of the boundary conditions applied (Coyle et al.[3] had to assume a slip coefficient), there were some uncertainties on the accuracy of their predicted film thickness. Indeed, there is a shift between what Coyle et al.[3] predicted and what they measured, however, the trends in the predictions with parameters variations fits the data well. Further proof of these predictions was given later by Hao and Haber[4] who used the same CFD method. As the data of Coyle et al.[3] were obtained from a model reverse roll coater (two rollers half submerged in a trough containing the coating liquid), limited in the range of operating conditions ($h_0 > 125$ μm and $V_A < 1$ m/s) and intended to track the changes of H_M with r_S and as they were not specifically concerned with how thin and fast the actual film thickness could be formed, it is desirable to provide further data to help validate and improve the theoretical approach they developed. The provision of further data from a typical (not a model) reverse roll coater is one aspect of the work presented in this article. It is important to note in

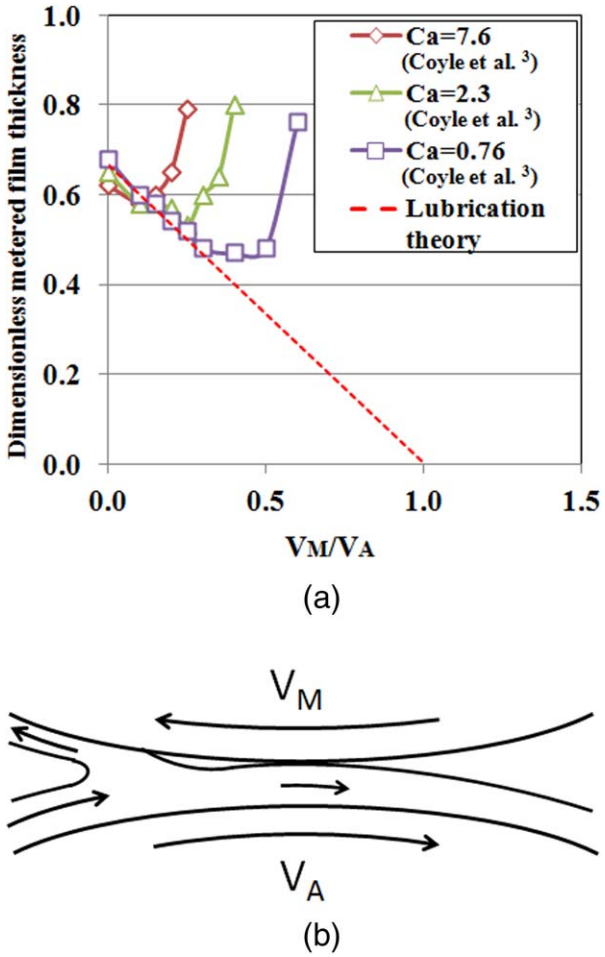

Figure 2. (a) Variation of experimental H_M with r_S as reported by Coyle et al.[3] and (b) Explanation by Coyle et al.[3] for the variation of H_M with r_S and the onset of cascade instabilities.

[Color figure can be viewed in the online issue, which is available at wileyonlinelibrary.com.]

this respect that Coyle et al.[3] also referred in their article to a pilot coater, which they used at gap heights of 25–250 μm and "noted that no stable, uniform flow region was observed on the pilot coater." The follow-up work of Kang and Liu[5] provided an experimental correlation for the critical speed ratio, r_S^* at which the minimum film thickness is observed as a function of Ca

$$r_S^* = 0.29\mathrm{Ca}^{-0.54} \tag{3}$$

Again, the Kang and Liu[5] data were limited to large gaps (200–800 μm) and low speeds ($V_A < 0.9$ m/s).

When considered in the light of experimental observations, Coyle et al.[3] explain that this upturn in film thickness with increasing speed ratio and the penetration of the dynamic wetting line inside the nip coincide with the onset of instabilities known as "cascade," "herringbones," or "seashores" which are the entrainment of cross-web bands of air resulting from the inability of the dynamic wetting line to move inside and passed the minimum gap position in a continuous, stable manner. What happens is that the line jumps between two unstable positions thus trapping these cross-web air bands in the process which periodically cushion themselves against the metered film causing it to show periodic transversal bars on its surface. These very large (of order of the gap size) air entrainment instability bars should not be confused with the saw-teeth shaped instabilities with microscopic air bubbles which occur in *all* coating flows as a result of dynamic wetting failure.[6–9] These dynamic wetting failure air entrainment instabilities are another limit to stable operation and together with cascade and another form of surface instabilities, ribbing define the stable operating coating window.

Ribbing instabilities, unlike cascade, are not unique to reverse roll coating. They manifest themselves in all coating flows but are particularly noted in forward roll coating where they occur at relatively low speeds, typically 0.5 m/s and less when viscous fluids are used. In forward roll coating, the applicator and metering rollers move in the same direction at the nip and a separation meniscus forms. It is this feature in the flow and the converging–diverging gap geometry that is primarily, responsible for the onset of ribbing instabilities as explained by Pearson.[10] These flow conditions create large positive pressure gradients in the downstream region approaching the separation meniscus and if the right surface tension forces are not applied to balance the viscous forces (low-capillary number Ca or high gap to radius ratio, h_0/R), there is a greater propensity for the meniscus to destabilize and become ribbed. Following Pitts and Greiller[11] original argument which was developed for forward roll coating and later formalized by Savage[12] to any cavity-fluid interface, the condition for stable flow is expressed by the following criterion

$$\frac{d}{dx}\left(p + \frac{\sigma}{R_C}\right) < 0 \tag{4}$$

Here, R_C is the radius of curvature of the meniscus and dp/dx is the gradient of the fluid pressure immediately upstream of the meniscus upon which ribbing may occur. When the above criteria is further developed in forward roll coating with the pressure variables explicitly expressed (see Benkreira et al.[13] or Coyle et al.[14]), the capillary number Ca and the gap to roll radius ratio H_0 ($=h_0/R$) appear naturally as parameters controlling the onset of instability. This is substantiated by much experimental data as represented in Figure 3 which correlates the onset of ribbing instabilities in terms of a critical $\mathrm{Ca_c}$ for a given H_0 as

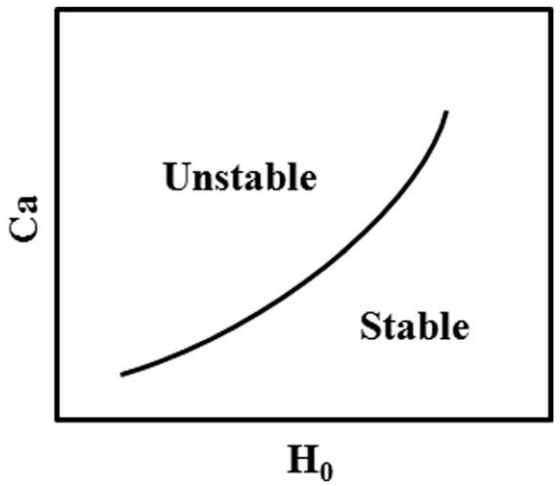

Figure 3. Ca vs. H_0 type of correlation for onset of ribbing in forward roll coating.[13,14]

$$Ca_c = \alpha(H_0)^{\beta} \quad (\alpha \text{ and } \beta \text{ are constants}) \tag{5}$$

As for reverse roll coating, no such correlation, experimental or theoretical has been identified. Following Eq. 4 and considering the lower pressures that develop in reverse roll coating as the speed ratio is increased (less fluid going through the nip will create less hydrodynamic pressure), it would be expected that reverse roll coating would be more resistant to ribbing instabilities to forward roll coating. This is well established as in practice reverse roll coating is preferred to forward roll coating. Conversely and in agreement with Eq. 4, it is to be expected that as the speed ratio is reduced there will be a point at which the balance of pressure and surface tension force will not hold, producing ribbing instabilities. This was observed in the experiments of Coyle et al.[3] and Reglat and Tanguy.[15] Neither group of workers gave an equation describing the onset of ribbing instabilities in reverse roll coating. Rather, Coyle et al.[3] provided graphical coating windows to illustrate the complex route to get to stable conditions in terms of manipulating Ca, r_S, and H_0. Furthermore, they found that when carrying out experiments with small gaps (25–250 μm) in a pilot reverse roll coater that the films produced were always unstable, either through cascade or ribbing. They gave for these conditions the following empirical criterion

$$Ca_c = 0.16(r_S)^{-2.16} \quad \text{with } 0.2 < Ca_c < 4 \text{ and } 25\ \mu\text{m} < h_0 < 250\ \mu\text{m} \tag{6}$$

Clearly, it follows from this observation that Coyle et al.[3] did not observe any stable films being formed below 250 μm in an actual reverse roll coater. Their model reverse roll coater (two rollers half submerged in a trough containing the coating liquid) also infers from the data at the lowest gap tested (125 μm) that stable films may not be obtainable at gaps smaller than 125 μm.

As for Reglat and Tanguy,[15] their operating conditions of very low-speed ratios (0.015– 0.12) rendered their films to be always unstable, not an important consideration in the practical application of coating article they were concerned with. However, by measuring the variation of maximum pressures in the nip and the heights of the ribs, they were able to establish that although the metering roll speed was much smaller in relation to the applicator speed it played a part in forming instabilities. They concluded interestingly that the Reynolds number ($Re_M = \rho V_M h_0/\mu$) based on the metering roller speed was a more appropriate descriptor of instabilities than Ca, the capillary number based on the applicator speed. The important conclusion with regard to ribbing instabilities in reverse roll coating is that they exist within a range of conditions but unlike in forward roll coating, they have not been correlated in *any* manner.

Having reviewed previous work on reverse roll coating and associated instabilities, it is the aim of this work to "push the limits" of this coating operation to produce the thinnest possible films (less than 10 μm wet) at speeds higher than current operations (1 m/s and higher if possible) by investigating the fluid mechanics of this operation near the lowest permissible gap.

Experimental Method

A reverse roll coater is a simple set-up, two rollers separated by a gap and rotating in opposite directions at the nip. The size and variation of the film thickness formed, however, depends strongly on maintaining the gap size and roller speeds constant with time. The rollers were thus machined accurately and set in a stiff steel frame in which the gap can be changed and controlled accurately. The drives were also designed carefully to provide constant rotation transmitted to the roller shafts. In addition, because visualization is important in determining the onset of instabilities, provisions of appropriate lighting were made to facilitate this.

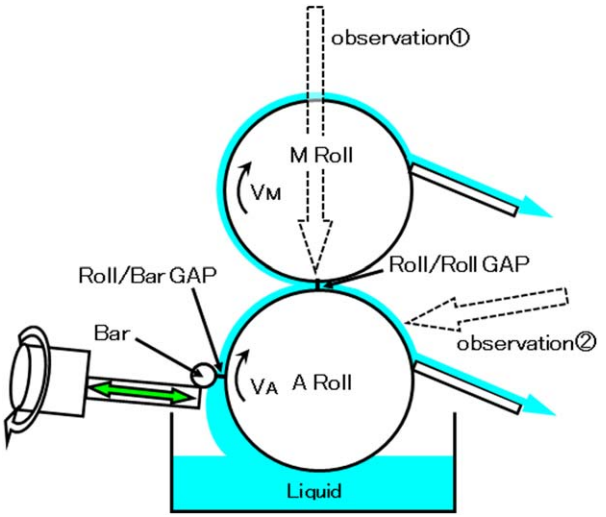

Figure 4. Schematic representation of the experimental set-up used.

[Color figure can be viewed in the online issue, which is available at wileyonlinelibrary.com.]

Two types of rollers were used: steel-steel for the measurements of film thickness and establishing the stability window and steel-transparent Perspex to observe the flow and the onset of instabilities. The steel rollers were 0.20 m long and 0.20 m in diameter, chromed and polished to provide an accuracy in the roller radius of $<\pm 2.5$ μm with a chrome finish of ± 0.1 μm. The transparent Perspex roller although machined to the highest standard had an eccentricity of ± 25 μm. This is because during machining the exposure of the Perspex to heat cannot produce a better finish.

For any given combination of rollers, the rollers pair were slotted and held in place in a stiff stainless steel frame, the design of which is shown schematically in Figure 4. The gaps between the rolls were set by placing shims accurate to ± 0.1 μm between the rolls bearing blocks and checked using slip gauges. Gaps of 200, 100, 50, and 25 μm were tested in this study. The rollers were driven independently by inverter-controlled AC geared motors via a combination of timing pulleys and belts. Initial calibration of the inverters provided accurate control of the roller speeds to ± 0.1 m/min. To facilitate feeding, the applicator roller was partially immersed in a trough but the film it picked up was further doctored and monitored using a gapped steel rod attached to a vernier.

As in practice, reverse roll does not allow for the return of the film on the metering roller, this film was wiped clean in our system using a scraper attached to a funneling device to enable collection for measurement if required.

The measurement of the metered film thickness was carried out using the simple but reliable method of scraping the

Table 1. Physical Properties of the Coating Fluids Used in This Study

Coating Fluids	Viscosity, μ (mPa s)	Surface Tension σ (mN/m)	Density ρ (g/cm^3)
Lub. Oil M5	6.6	26.8	0.82
Lub. Oil M15	27	28.2	0.86
Lub. Oil M68	176	28.6	0.87
Glycerol	5.9	65.4	1.13

film off the roller and weighting it. The accuracy was improved by carrying out the scraping over a reasonably long period of time, between 30 and 120 s, depending on the amount of the metered liquid. In all cases, the measurements were repeated and the result averaged, giving the accuracy in the film thickness of $\pm 3\%$.

Detection of ribbing, cascade, and other instabilities was carried out with the naked eye (in actual practice this is the test) using strong but cold illumination so as not to heat the set-up and coating fluids. By ramping up and down the speed near the critical conditions, an accurate measurement of the onset of instabilities can be obtained to within ± 0.2 m/min. The experiments with the Perspex roller enabled the observation of the flow in the nip region, particularly the position and the shape of the separation meniscus. This visualization was achieved by focusing a TK-1270 Colour video camera (JVC) coupled with a Canon Macro lens (50 mm, 1:3.5) directly above the Perspex metering roller and mounted on an accurately moveable *x-y-z* platform. The images captured by the camera were stored directly into a PC with software (Compro DTV4). The setup was properly calibrated by first determining the degree of magnification of the image captured using a photograph of a graticule placed in the gap between the rollers.

The design of the experiments was guided by the findings from prior work which indicates as discussed above that small gaps h_0 coupled with low capillary number Ca and high speed ratios r_S were required to produce the thinnest possible uniform thickness films at the highest possible speeds. One immediate implication is in the choice of the coating liquid viscosity which is required hence our choice of fluids in the range decreased from 176 to 7 mPa s. With regard to both density and surface tension, the choice is limited and surface tensions in the range 27–65 mN/m and densities in the range 820–1130 kg/m^3 were considered. Four coating fluids were tested: three lubricating oils and one water–glycerine solution which covered viscosities, surface tensions and densities at 20°C in the range given above (see Table 1). The surface tensions were measured using the FTA 188 video tension meter which operates on the principle of creating a drop pending from a syringe, recording a series of pictures of the pendant drops to obtain a volume and a weight of the pendant drop from which the surface tension can be calculated from a force balance. Viscosities were measured using a Physica MCR 301, Anton Paar rheometer operating in shear mode in a cone and plate geometry over a wide range of shear rates 0–1500 s^{-1}. The rheological testing established that all the fluids tested were Newtonian over the range of processing conditions deployed.

Results and Discussion

A general point in the presentation of the data is that by necessity they are given in dimensional form to assess how thin and how fast the films were produced and in dimensionless form to compare with the experimental and theoretical predictions of Coyle et al.[3] Crucially, the theoretical predictions of Coyle et al.[3] infer that the onset of cascade coincides with the critical speed ratio r_S* at which the upturn in film thickness is observed. No theoretical criterion is available for the onset of instability.

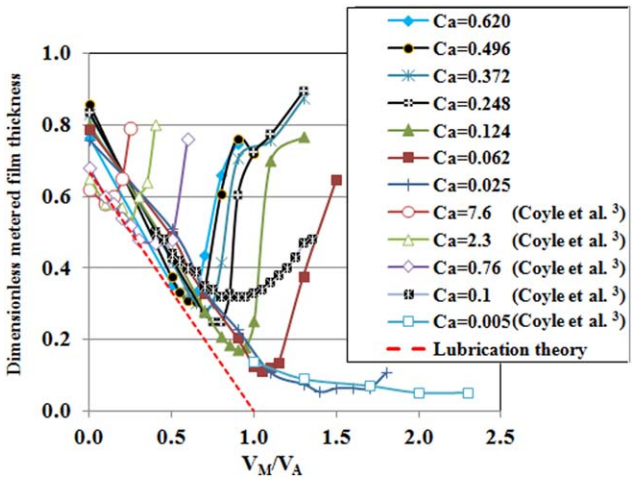

Figure 5. Film thickness measured in this study and comparison with data of Coyle et al.[3]

[Color figure can be viewed in the online issue, which is available at wileyonlinelibrary.com.]

Film thickness

The film thickness data are presented in Figure 5 as H_M vs. r_S at fixed Ca for comparison with the only other available data of this kind, those due to Coyle et al.[3] The first observation is the qualitative agreement regarding the form of the curve, a linear lubrication approximation region followed by an upturn above a critical speed ratio, r_S^*. The second observation is the added value of the present work: it provides complementary data in the interesting region where the film thickness drops significantly below 0.45 down to as low as 0.05. It is seen in Figure 5 that the bulk of Coyle et al.[3] data were in the higher range of film thickness, except for two data sets at $Ca = 0.1$ and $Ca = 0.005$. If the comparison is examined further (see Figure 6), it is observed that the measured minimum film thicknesses at low Ca are consistently lower than those of Coyle et al.[3] by about 30%. Interestingly, when both sets of data are compared with the theoretical predictions made by Coyle et al.,[3] a closer fit to the data measured here is observed (see Figure 7). Remarkably, in both sets of data and in the theoretical predictions, for a given capillary number, the critical speed ratios where the minimum film thickness occurs are similar (see Figures 7 and 8). As the data of the present study were obtained from a *typical* reverse roll coating configuration, the discrepancy, albeit minor but significant, suggests that the *half submerged* configuration stated by Coyle et al.[3] as being "a good representation of the flow in a reverse roll coater" is strictly not accurate. This is not surprising as the critical speed ratio and the minimum film thickness are critically related to the flow near the minimum gap position. Recall that according to Coyle et al.,[3] the critical speed ratio condition signals that the dynamic wetting line has been pulled through the gap. While in this study's configuration, there is no flow

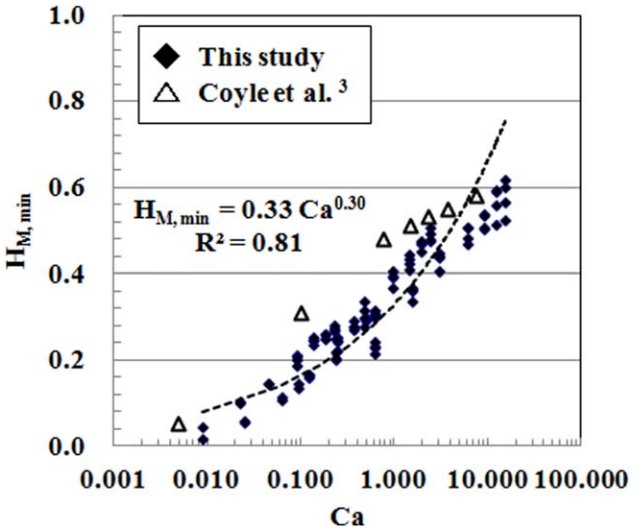

Figure 6. Minimum film thickness measured in this study (◆) and comparison with data of Coyle et al.[3] (△).

[Color figure can be viewed in the online issue, which is available at wileyonlinelibrary.com.]

opposition to this situation occurring, in Coyle et al.[3] flow geometry, the rollers are half-submerged constraining somewhat the separation flow. Although the surplus of liquid in the half submerged case may not restrict the movement of the dynamic wetting line, that is, the onset of the critical speed ratio, it could affect the flux of liquid taken by the applicator roller, increasing it comparatively with the unsubmerged case. The film thicknesses measured by Coyle et al.[3] in an actual coater, similar to our arrangement, under starved feeding demonstrate clearly that the feeding conditions have an effect on the thickness of the films formed.

In conclusion, the better fit between this study's data and the theoretical predictions reinforces the suggestion that the half submerged configuration is not an accurate representation of the actual reverse roll coating flow. This makes the data presented here all the more important for the more accurate design and operation of actual reverse roll coating. An experimental correlation on how the minimum film thickness varies with Ca and r_S can also be developed to guide

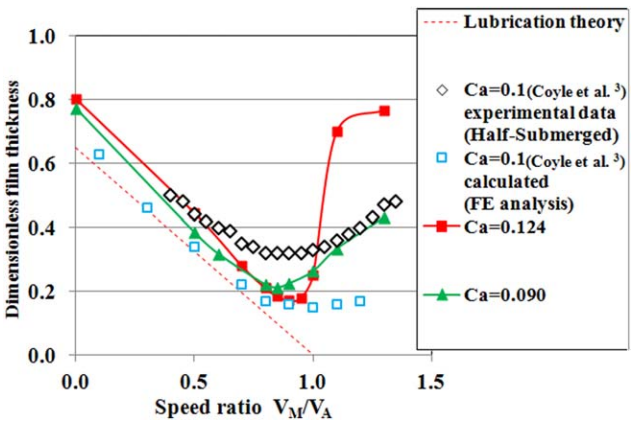

Figure 7. H_M measured in this study compared with H_M measured and predicted by Coyle et al.[3]

[Color figure can be viewed in the online issue, which is available at wileyonlinelibrary.com.]

operation. This correlation derives from the data given in Figure 6 and can be expressed as

$$H_{M,min} = 0.33Ca^{0.30} \tag{7}$$

Also, as the critical speed ratio r_S^*, where the upturn in film thickness occurs is an important indicator of stability and a limit for a lubrication approximation analysis (linearity of H_M with r_S), the critical speed ratio r_S^* was correlated with Ca and this finding compared with that of Kang and Liu[5] (Eq. 3). Figure 8 shows the comparison and suggests a more appropriate correlation covering the wide range of Ca tested as

$$r_S^* = 0.46Ca^{-0.32} \tag{8}$$

Another important point to note with these data is that they provide answers to the challenges set at the outset with regard to producing very thin films at high speeds. To illustrate this, the data is presented in dimensional form as in Figure 9 which gives a typical set of data obtained at the lowest permissible positive gap of 25 μm with a coating of viscosity 7 mPa s and surface tension of 27 mN/m. A minimum film thickness of 7.5 μm is obtained here at speeds of 2.5 m/s. This shows clearly the potential of reverse roll coating at producing very thin films when operated at near zero gaps. Films thinner than 7.5 μm are permissible if the applicator speed is lowered and an appropriate speed ratio (below the critical value) is used. Now the question is: are these films uniform, that is, is the flow stable at these conditions?

Instability

As explained in Introduction, two forms of surface instabilities can arise: ribbing which is common to all coating flows and cascade which is specific to reverse roll coating. Prior to the article of Coyle et al.,[3] none of these instabilities had been reported with reverse roll coating so their findings

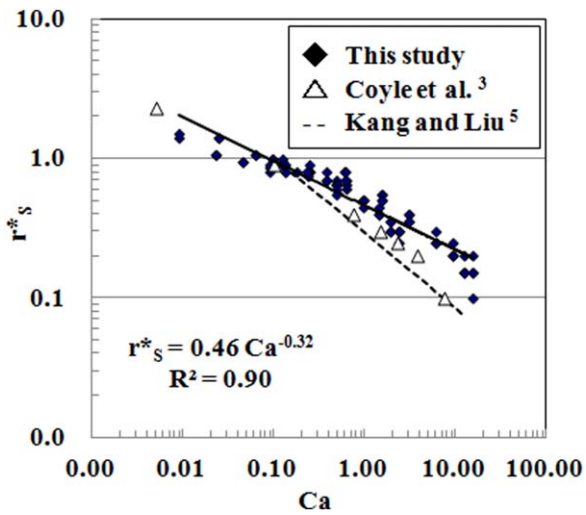

Figure 8. Critical speed ratio vs. Ca: data from this study (◆) and comparison with Coyle et al.[3] data (△) and Kang and Liu[5] correlation (-------).

[Color figure can be viewed in the online issue, which is available at wileyonlinelibrary.com.]

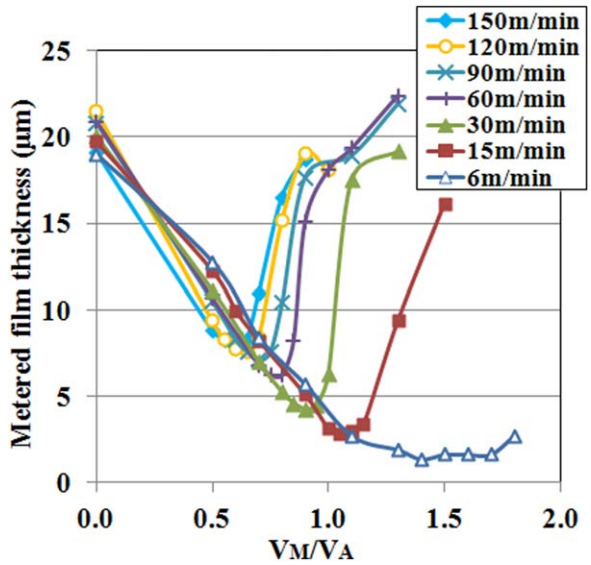

Figure 9. Feasibility of producing thin films with reverse roll coating ($h_0 = 25$ μm; $\mu = 6.6$ mPa s, and $\sigma = 26.8$ mN/m).

[Color figure can be viewed in the online issue, which is available at wileyonlinelibrary.com.]

are used as a first basis of comparison. These show that the parameters controlling the stable coating window, situated between regions of ribbing and cascade, are the capillary number Ca ($=\mu V_A/\sigma$), the speed ratio, r_S ($=V_M/V_A$), and the dimensionless metering gap h_0/R. With large gaps, the region Ca vs. r_S delimiting the stable coating window is broad and shows that for any given Ca it is always possible to eliminate ribbing by increasing the speed ratio before eventually entering the cascade region. As the gap is reduced, the stable coating window shrinks and the range of speed ratio necessary for stable flow before cascade sets in narrows, until below a critical gap the flow becomes unstable at all Ca and r_S. The data at gaps of 200, 100, 50, and 25 μm and viscosities 27 and 176 mPa s shows this behavior but also reveals some additional features at high Ca (>4) not covered in the work of Coyle et al.[3] One such a feature is that at gaps equal to 25 μm and 50 μm an upper limit in Ca was observed above which no stable flow occurs whatever the speed ratio is set at and the flow change directly from ribbing into cascade (see Figure 10b and c) or always ribbing (see Figure 10a). A second feature is that with the fluid of viscosity 27 mPa s, at all gaps 25, 50, 100, and 200 μm, the flow goes ribbing-stable-ribbing-cascade (see Figure 10b), whereas the fluid of viscosity 176 mPa s always goes ribbing-stable-cascade (see Figure 10c). This can be explained with reference to the movement of the wetting line towards the minimum gap as Ca and r_S are increased. With the high-viscosity liquid or Ca, it is closer to the minimum gap position than with the low-viscosity fluid or Ca and as the speed ratio is increased, it moves past the minimum gap and induces cascade. With the low-viscosity fluid, it remains shifted away from the minimum gap position so becomes prone to ribbing instead as the speed ratio is increased until with further increase in speed ratio it goes past the minimum position and triggers cascade instabilities. These observations are consistent with the CFD simulations of Coyle et al.[3] on the movement of the wetting line towards the minimum gap as Ca and r_S are increased.

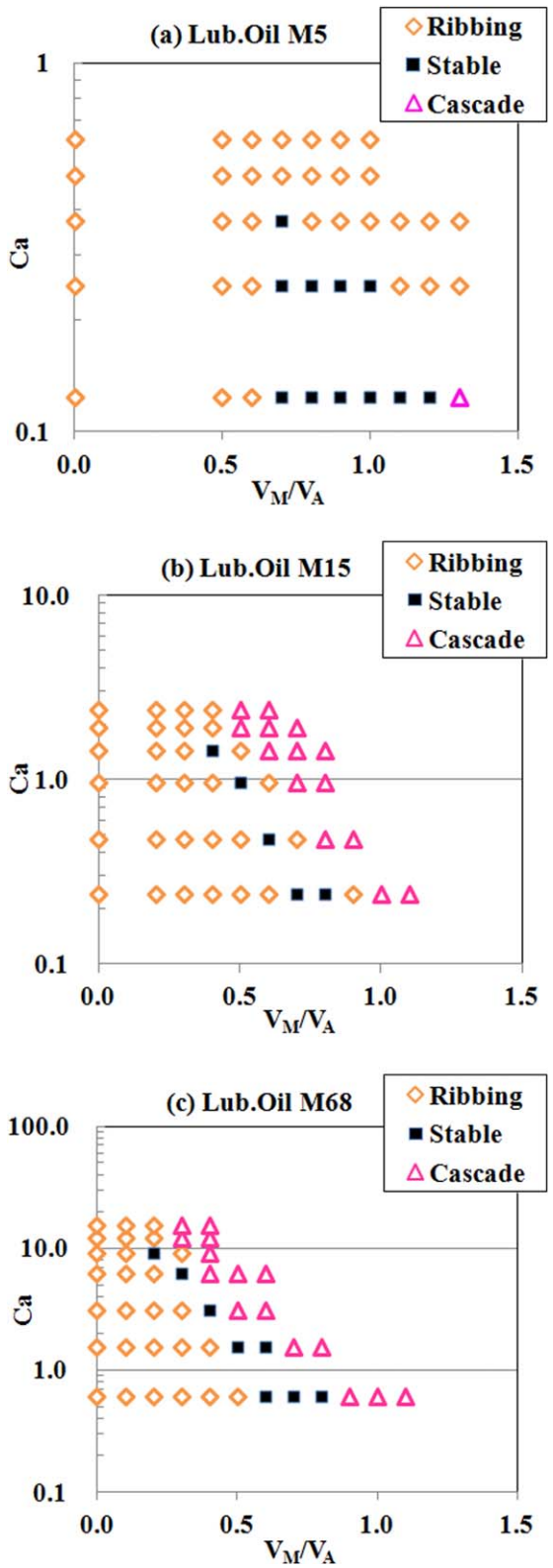

Figure 10. (a) Coating window (Lub. oil M5, Roll gap = 50 μm, supply film = 200 μm); (b) Coating window (Lub. oil M15, Roll gap = 50 μm, supply film = 200 μm); and (c) Coating window (Lub. oil M68, Roll gap = 50 μm, supply film = 200 μm).

[Color figure can be viewed in the online issue, which is available at wileyonlinelibrary.com.]

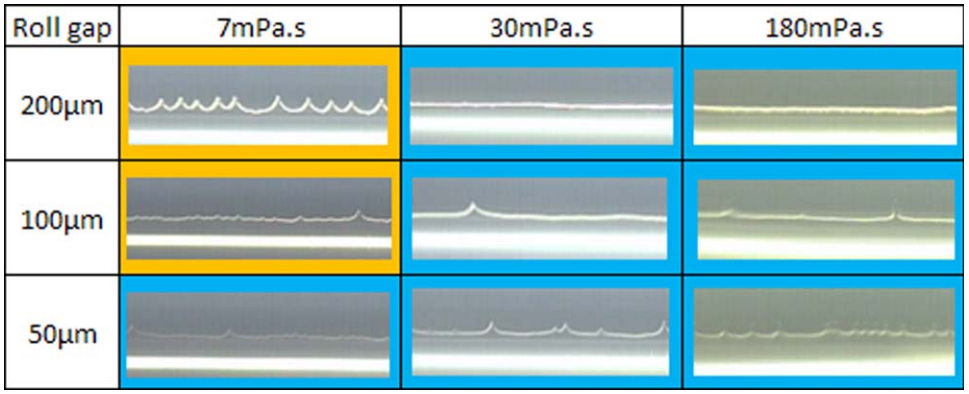

Figure 11. Popensity for ribbing instabilities is reduced as the gap size is decreased rather than being exacerbated as in the case of the high viscosity fluids.

[Color figure can be viewed in the online issue, which is available at wileyonlinelibrary.com.]

The behavior just discussed with regard to viscosity suggests that a different effect was beginning to be observed in the experiments at the lower viscosity of 27 mPa s. This observation brings into consideration the important work of Reglat and Tanguy[15] on instabilities in the metering-size press flow for the treatment of paper, a flow that resembles reverse roll coating, except that it is driven at very much higher speeds (applicator speed of 1000 m/min and metering speed of 300 m/min), with very low-viscosity fluids (20 mPa s) and in small gaps (<40 μm). Reglat and Tanguy[15] confirmed the role of Ca and r_S in the control of ribbing instabilities but expressed in terms of rib widths only. Rib heights, which are the features most discernible, could only be differentiated by the inertia effect as expressed by a Reynolds number based on the metering roller speed ($\mathrm{Re} = \rho V_m h_0/\mu$). In reverse roll coating operations, the conditions are normally less severe (applicator speed $<$ 1–2 m/s; viscosity $>$ 100 mPa s; gaps >50 μm) than in a metering size press and the inertia effect may be considered negligible. However, with 27 mPa s and speeds in excess of 2 m/s, the conditions are close to those where inertia effects may well be important so as to change completely the onset of instabilities, ribbing in particular (see theoretical discussion in Coyle et al.[14] on stabilization of ribbing by inertia effects). Such observations called for experiments at even lower viscosities than 27 mPa s so as to enhance the inertia effect further. Figure 11 shows such data with a fluid of viscosity 7 mPa s in comparison with fluids of higher viscosities at the critical coating flow conditions where ribbing instabilities arise. Interestingly, it is observed that the propensity for ribbing instabilities is reduced as the gap size is decreased rather than being exacerbated as in the case of the high viscosity fluids.

Clearly, ribbing in this 7 mPa s case is being controlled in a way different from that normally encountered, that is, not by applicator roller Ca or the capillary forces generated. We are thus justified in assuming that in this situation, the other forces at play—inertia forces generated by the applicator roller—are the destabilizing factor. As in all cases, surface tension stabilizes the flow, the applicator roller Weber number, We ($=\rho V_A h_0^2/\sigma$) is the appropriate parameter to

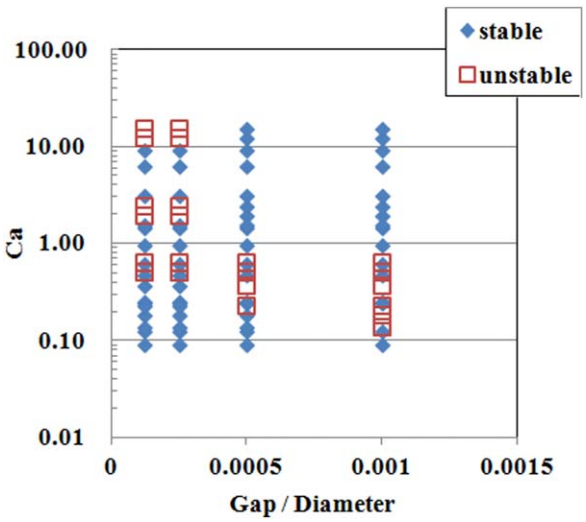

Figure 12. Ribbing instabilities as correlated using Ca: poor fit.

[Color figure can be viewed in the online issue, which is available at wileyonlinelibrary.com.]

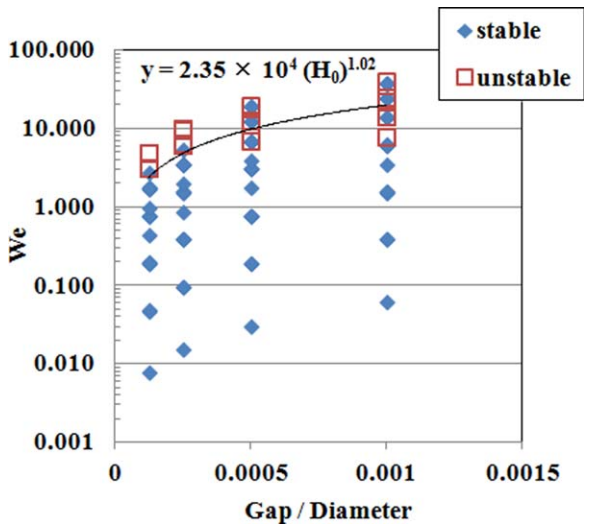

Figure 13. Ribbing instabilities as correlated using We: good fit.

[Color figure can be viewed in the online issue, which is available at wileyonlinelibrary.com.]

consider as an alternative to the applicator roller Ca. To test this hypothesis, these data were processed for all conditions (i.e., including low and large viscosities) with respect to Ca in Figure 12 and We in Figure 13. The better fit with We proves indeed that it is the case that in reverse roll coating it is the applicator roller We number and not the applicator roller Ca number that is the control parameter of ribbing instabilities. The best fit correlation of all the data describing the onset of instability is given by

$$\mathrm{We} = 2.35 \times 10^4 (H_0)^{1.02} \tag{9}$$

Conclusions

An experimental study replicating reverse roll coating has been carried out to assess the feasibility of this coating technique to produce very thin films (<10 μm) at high speed (>1 m/s) which are uniform. The data obtained with a series of fluids and in a range of gaps show that such stable films can be achieved by using low-viscosity fluids (<10 mPa s) and operating at the smallest gaps permissible (~ 25 μm). Unexpectedly, these conditions of low viscosities and small gaps stabilize the flow and offer the potential to apply this rather rudimentary coating technique to the newer technological applications, for example, solar cells and plastic electronics. More generally, the data obtained complement earlier experimental work on reverse roll coating which oddly has been limited despite the wide utilization of this technique. These data also provide a platform for developing further theoretical predictions of the kind first presented by Coyle et al.[3] Finally and importantly, unlike forward roll coating where instabilities are governed in a coating window depicted by applicator roller Ca vs. dimensionless gap, this study shows that it is the applicator roller We number and not the applicator roller Ca which is the critical parameter in reverse roll coating.

Acknowledgments

The authors acknowledge the support of the Films R&D Centre of Toyobo Co. Ltd., Otsu, Japan and of the Thin Films Research Group of the University of Bradford, UK.

Literature Cited

1. Ho WS, Holland FM. Between-roll metering coating technique, a theoretical and experimental study. *TAPPI*. 1978;61:53–56.
2. Benkreira H, Edwards MF, Wilkinson WL. Roll coating of purely viscous liquids. *Chem Eng Sci*. 1981;36:429–434.
3. Coyle DJ, Macosko CW, Scriven LE. The fluid dynamics of reverse roll coating. *AIChE J*. 1990;36:161–174.
4. Hao Y, Haber S. Reverse roll coating. *Int J Numer Methods Fluids*. 1999;30:635–652.
5. Kang YT, Liu TJ. Minimum film thickness for reverse roll coating. *Chem Eng Sci*. 1991;46:2958–2960.
6. Deryagin BM, Levi SM. Film Coating Theory. London: Focal Press, 1964.
7. Gutoff EB, Kendrick CE. Dynamic contact angles. *AIChE J*. 1982;28:459–466.
8. Blake TD, Ruschak KJ. Wetting static and dynamic contact Lines. In: Kistler F, Schweizer PM, editors. Liquid Film Coating. London: Chapman & Hall, 1997:63–97.
9. Benkreira H. Experimental study of dynamic wetting in reverse-roll coating. *AIChE J*. 2002;48:221–226.
10. Pearson JRA. The instability of uniform viscous flow under rollers and spreaders. *J Fluid Mech*. 1960;7:481–500.
11. Pitts E, Greiller J. The flow of thin liquid films between rollers. *J Fluid Mech*. 1961;11:33–51.
12. Savage MD. Cavitation in lubrication: 2. Analysis of wavy interfaces. *J Fluid Mech*. 1997;80:757–767.
13. Benkreira H, Edwards MF, Wilkinson WL. Ribbing instability in the roll coating of Newtonian fluids. *Plastic Rubber Proc. Appl*. 1982;2:137–144.
14. Coyle DJ, Macosko CW, Scriven LE. Stability of symmetric film-splitting between counter-rotating cylinders. *J Fluid Mech*. 1990;216:437–458.
15. Reglat O, Tanguy PA. Experimental study of the flow nip of a metering-size in the metering press. *AIChE J*. 1997;43:2911–2920.

Manuscript received July 26, 2012, and revision received Oct. 2, 2012.